Crystal Structures and Luminescence Properties of Platinum(II) Complexes Containing 3,3′-Biisoquinoline

Masako Kato,*[1a] Kumiko Sasano,[1a] Chizuko Kosuge,[1a] Mikio Yamazaki,[1b] Shigenobu Yano,[1a] and Masaru Kimura[1a]

Department of Chemistry, Faculty of Science, Nara Women's University, Nara 630, Japan, and Rigaku Corporation, Akishima, Tokyo 196, Japan

Received June 7, 1995[⊗]

Three new platinum complexes containing 3,3′-biisoquinoline (*i*-biq), $[Pt(CN)_2(i\text{-biq})]$ (**1**), $[PtCl_2(i\text{-biq})]$ (**2**), and $[Pt(i\text{-biq})_2](PF_6)_2$ (**3**), have been synthesized as orange-red, yellow, and colorless crystals, respectively. Their crystal structures and luminescence properties are reported. Crystal data: for **1**·0.5H_2O, $PtO_{0.5}N_4C_{20}H_{13}$, orthorhombic, *Pbcm*, $a = 13.989(2)$ Å, $b = 18.304(1)$ Å, $c = 6.682(3)$ Å, $V = 1710.9(6)$ Å^3, $Z = 4$, and final $R = 0.039$ ($R_w = 0.033$) for 970 independent reflections; for **2**·DMF·H_2O, $PtCl_2O_2N_3C_{21}H_{21}$, triclinic, $P\bar{1}$, $a = 11.047(1)$ Å, $b = 12.397(3)$ Å, $c = 8.000(2)$ Å, $\alpha = 106.56(1)°$, $\beta = 100.15(1)°$, $\gamma = 76.15(1)°$, $V = 1012.8(3)$ Å^3, $Z = 2$, and final $R = 0.058$ ($R_w = 0.077$) for 4219 independent reflections; for **3**·2DMF, $PtP_2F_{12}O_2N_6C_{42}H_{38}$, triclinic, $P\bar{1}$, $a = 10.795(2)$ Å, $b = 13.511(2)$ Å, $c = 8.281(1)$ Å, $\alpha = 105.22(1)°$, $\beta = 112.17(1)°$, $\gamma = 85.02(1)°$, $V = 1079.2(3)$ Å^3, $Z = 1$, and final $R = 0.038$ ($R_w = 0.042$) for 3606 independent reflections. Square-planar complexes of **1** are stacked in the crystal to form a columnar structure with the Pt−Pt distance of 3.34 Å. The crystal emits strongly, even at room temperature, and the emission spectrum is similar to that for the $[Pt(CN)_2(bpy)]$ crystal (bpy = 2,2′-bipyridine), which is due to a $^3d\pi^*[d\sigma^*(Pt) \rightarrow \pi^*(i\text{-biq})]$ transition. The single crystal emission spectrum at 77 K is, however, observed as a superposition of broad $^3d\pi^*$ and sharp $^3\pi\pi^*(i\text{-biq})$ emissions. The crystal structure of **2** has a completely different stacking structure from that of **1**. The stacking occurs on the *i*-biq ligands, and the Pt atoms are separated more than 6 Å. The complex exhibits only a structured emission component assigned to the $^3\pi\pi^*(i\text{-biq})$ transition in the crystal at 77 K, in agreement with the crystal structure with no Pt−Pt interaction. In the crystal of **3**, the $[Pt(i\text{-biq})_2]^{2+}$ complexes are stacked but offset, being in close contact between parts of adjacent *i*-biq ligands. There is no Pt−Pt interaction also in this case. Two *i*-biq ligands in the complex are distorted to adopt the bowed conformation due to the steric crowding of the α-hydrogens on opposite ligands. Nevertheless, **3** provides almost the same $^3\pi\pi^*$ emission spectrum as **1** and **2** in dilute glassy solution at 77 K. The $^3\pi\pi^*$ emission spectra observed in the crystals of these Pt(II) complexes are red-shifted compared with those in dilute glassy solution. The fact is attributable to the $\pi-\pi$ intermolecular interactions between the ligands in the crystals. The factors controlling the crystal structures for these complexes are also discussed.

Introduction

It is well-known that square-planar platinum complexes have a tendency to stack in solid state and to show characteristic optical and electrical properties. When α-diimines such as 2,2′-bipyridine (bpy) are used as ligands, a variety of intermolecular interactions are expected, for example, metal−metal interaction and ligand $\pi-\pi$ interaction. In fact, polymorphism often occurs for platinum complexes, and the color and the emission behavior depend on the crystal structure and thus the intermolecular interaction.[2] $[PtCl_2(bpy)]$ is a typical complex, taking two crystal forms which are called yellow and red forms.[3] The red form has a stacked structure with platinum−platinum interaction (Pt···Pt = 3.45 Å), while the yellow form has no Pt−Pt stacking but has a stack on one pyridine ring of the bpy ligand.[4] They are interconverted to each other under various conditions.[5] Thus, it is interesting to explore the factors determining significant features of this kind of platinum complex and to control them.

3,3′-Biisoquinoline (*i*-biq) is an α-diimine with a larger π-system than 2,2′-bipyridine, while it has comparable σ-donor ability to bpy.[6] $[Ru(i\text{-biq})_3]^{2+}$ was reported to be the first

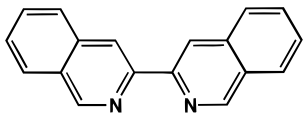

i-biq

example of ruthenium(II) complexes exhibiting triplet ligand-centered ($^3\pi\pi^*$) emission.[7] In contrast to the sharp $^3\pi\pi^*$ emission spectrum in dilute glassy solution, we observed a broad and red-shifted emission spectrum of the complex in the crystal state at 77 K.[8] On the basis of the X-ray crystal structure and the concentration dependence of the emission spectrum, the

⊗ Abstract published in *Advance ACS Abstracts,* December 1, 1995.

(1) (a) Nara Women's University. (b) Rigaku Corp.

(2) (a) Houlding, V. H.; Miskowski, V. M. *Coord. Chem. Rev.* **1991**, *111*, 145. (b) Thomas, T. W.; Underhill, A. E. *Chem. Soc. Rev.* **1972**, *1*, 99.
(3) Morgan, G. T.; Burstall, F. H. *J. Chem. Soc.* **1934**, 965.
(4) (a) Canty, A. J.; Skelton, B. W.; Traill, P. R.; White, A. H. *Aust. J. Chem.* **1992**, *45*, 417. (b) Osborn, R. S.; Rogers, D. *J. Chem. Soc., Dalton Trans.* **1974**, 1002. (c) Herber, R. H.; Croft, M.; Coyer, M. J.; Bilash, B.; Sahiner, A. *Inorg. Chem.* **1994**, *33*, 2422.
(5) Bielli, E.; Gidney, P. M.; Gillard, R. D.; Heaton, B. T. *J. Chem. Soc., Dalton Trans.* **1974**, 2133.
(6) Juris, A.; Barigelletti, F.; Balzani, V.; Belser, P.; von Zelewsky, A. *Inorg. Chem.* **1985**, *24*, 202.
(7) Belser, P.; von Zelewsky, A.; Juris, A.; Barigelletti, F.; Tucci, A.; Balzani, V. *Chem. Phys. Lett.* **1982**, *89*, 101.
(8) Kato, M.; Sasano, K.; Kimura, M.; Yamauchi, S. *Chem. Lett.* **1992**, 1887.

0020-1669/96/1335-0116$12.00/0

Table 1. Crystallographic Data

	$[Pt(CN)_2(i\text{-biq})]\cdot 0.5H_2O$	$[PtCl_2(i\text{-biq})]\cdot DMF\cdot H_2O$	$[Pt(i\text{-biq})_2](PF_6)_2\cdot 2DMF$
formula	$PtO_{0.5}N_4C_{20}H_{13}$	$PtCl_2O_2N_3C_{21}H_{21}$	$PtP_2F_{12}O_2N_6C_{42}H_{38}$
fw	513.45	613.41	1143.82
crystal system	orthorhombic	triclinic	triclinic
space group	*Pbcm* (No.57)	$P\bar{1}$ (No.2)	$P\bar{1}$ (No.2)
a, Å	13.989(2)	11.047(1)	10.795(2)
b, Å	18.304(1)	12.397(3)	13.511(2)
c, Å	6.682(3)	8.000(2)	8.281(1)
α, deg	90	106.56(1)	105.22(1)
β, deg	90	100.15(1)	112.17(1)
γ, deg	90	76.15(1)	85.02(1)
V, Å^3	1710.9(6)	1012.8(3)	1079.2(3)
Z	4	2	1
T, °C	25	25	25
λ, Å	0.71073	0.71073	0.71073
ρ_{obsd}, g·cm^{-3}	1.99	2.01	1.75
ρ_{calcd}, g·cm^{-3}	1.99	2.01	1.76
μ(Mo Kα), cm^{-1}	81.81	71.87	34.09
no. observns ($I > 3.00\sigma(I)$)	970	4219	3606
no. variables	174	253	358
R, R_w[a]	0.039, 0.033	0.058, 0.077	0.038, 0.042

[a] $R = \sum||F_o| - |F_c||/\sum|F_o|$; $R_w = [\sum w(|F_o| - |F_c|)^2/\sum w|F_o|^2]^{1/2}$, $w = 1/\sigma^2(F_o)$.

characteristic emission of the crystal was attributed to $\pi-\pi$ interactions between the *i*-biq ligands of the adjacent complexes. Thus, *i*-biq would be a useful ligand in particular for investigating the effect of the π-system.

In this work, we have prepared three new platinum(II) complexes, $[Pt(CN)_2(i\text{-biq})]$ (**1**), $[PtCl_2(i\text{-biq})]$ (**2**), and $[Pt(i\text{-biq})_2](PF_6)_2$ (**3**), and their X-ray crystal structures and luminescence properties have been investigated. On the basis of the results, we discuss the variation of the crystal structures constructed with the square-planar platinum complexes containing such an extended π-system and the effect of intermolecular interactions on the emissive state.

Experimental Section

Materials. 3,3′-Biisoquinoline was prepared according to the literature;[9] mp 205−206 °C. $K_2[PtCl_4]$ and NH_4PF_6 were purchased from Wako Pure Chemical Industries Ltd. Spectroscopic grade solvents was used for solution spectra.

Preparation of $[Pt(CN)_2(i\text{-biq})]$ (1). The complex was prepared by the method similar to that of the corresponding bpy complex, $[Pt(CN)_2(bpy)]$.[10] A 20% aqueous ammonia solution (40 mL) of 0.65 g of $Pt(CN)_2\cdot xH_2O$, which was obtained by thermal decomposition of $(NH_4)_2[Pt(CN)_4]$,[11] was added dropwise to a refluxing *N*,*N*-dimethylformamide (DMF) solution (40 mL) of 0.5 g of *i*-biq (2 mmol). Orange-red solid began to precipitate soon. The solution was further refluxed for 4 h. After cooling to room temperature, the orange-red product was collected; yield 60%. Orange-red plate crystals were obtained by the recrystallization from DMF. Anal. Calcd for $PtN_4C_{20}H_{12}\cdot 0.5H_2O$ (**1**·$0.5H_2O$): C, 46.88; H, 2.56; N, 10.93. Found: C, 46.30; H, 2.51; N, 10.89.

Preparation of $[PtCl_2(i\text{-biq})]$ (2). $K_2[PtCl_4]$ (5 mmol) was dissolved in water (130 mL). To the solution, 2 N HCl (10 mL) and then a suspension of *i*-biq (5 mmol) in acetonitrile (130 mL) were added. The mixture was heated with stirring for 1.5 h. The color of the suspended solution changed from red-orange to yellow. After cooling to room temperature, deposited yellow product was collected and recrystallized from DMF to give yellow needle crystals; yield 50%. Anal. Calcd for $PtCl_2N_2C_{18}H_{12}\cdot ONC_3H_7$ (**2**·DMF): C, 42.47; H, 3.15; N, 7.28. Found: C, 42.36; H, 3.22; N, 7.06.

Preparation of $[Pt(i\text{-biq})_2](PF_6)_2$ (3). A solution of **2** (1 mmol) and *i*-biq (1 mmol) in acetonitrile/water (1:1 (v/v), 500 mL) was refluxed for 5 h. After cooling to room temperature, the solution was filtered, and then an aqueous solution of excess amounts of NH_4PF_6 was added to the filtrate. Deposited yellowish white precipitate was collected; yield 50%). Colorless needle crystals were obtained from the recrystallization from DMF. Anal. Calcd for $PtP_2F_{12}N_4C_{36}H_{24}\cdot 2ONC_3H_7$ (**3**·2DMF): C, 44.10; H, 3.35; N, 7.35. Found: C, 44.18; H, 3.39; N, 7.33.

Collection and Reduction of X-ray Diffraction Data. The X-ray diffraction data were obtained on a Rigaku AFC-7R four-circle diffractometer with graphite monochromated Mo Kα radiation and a 18 kW rotating anode generator. An orange-red plate crystal of **1**, a yellow prismatic crystal of **2**, and a colorless plate crystal of **3** having appropriate dimensions of 0.18 × 0.10 × 0.02 mm, 0.22 × 0.20 × 0.14 mm, and 0.22 × 0.16 × 0.04 mm, respectively, were mounted on glass fibers. The data were collected using the $\omega-2\theta$ scan technique to a maximum 2θ value of 55° at a speed of 8, 16, and 16°/min (in ω) for **1**, **2**, and **3**, respectively. The weak reflections ($I < 10.0\sigma(I)$) were rescanned (maximum of four scans), and the counts were accumulated to ensure good counting statistics. The intensities of three standard reflections were monitored at 150-reflection intervals. For all the complexes, fluctuations for the F_o values were less than 1% during the data collection. Index ranges are as follows: $-18 \le h \le 0$, $-19 \le k \le 0$, $0 \le l \le +8$ for **1**; $-14 \le h \le +14$, $-15 \le k \le +15$, $-10 \le l \le 0$ for **2**; $-14 \le h \le 0$, $-17 \le k \le +17$, $-9 \le l \le +9$ for **3**. A total of 2289 reflections was collected for **1**. Of the 5004 reflections which were collected for **2**, 4667 were unique ($R_{int} = 0.010$), and of the 5241 reflections measured for **3**, 4980 were unique ($R_{int} = 0.036$). An empirical absorption correction based on azimuthal scans of several reflections was applied, which resulted in transmission factors in ranges 0.41−1.00, 0.75−1.00, and 0.75−1.00, for **1**, **2**, and **3**, respectively. The data were corrected for Lorenz and polarization effects. As for **2**, a correction for secondary extinction was applied (coefficient = $1.47616e^{-6}$). Pertinent crystallographic parameters are summarized in Table 1.

Solution and Refinement of the Structures. All the structures were solved by direct methods[12] and expanded using Fourier techniques. The non-hydrogen atoms were refined anisotropically. For the analysis of **1**, all atoms are initially located on the mirror plane ($z = 0.25$). As the refinement proceeded, however, it turned out that a thermal ellipsoid of several atoms became extraordinarily elongated along the normal to the mirror plane. Thus, C14−C17 atoms were refined without a fix on the mirror plane as disordered atoms with the occupancy factors of

(9) Belser, P.; von Zelewsky, A.; Juris, A.; Barigelletti, F.; Balzani, V. *Gazz. Chim. Ital.* **1985**, *115*, 723.
(10) Che, C.-M.; He, L.-Y.; Poon, C.-K.; Mak, T. C. W. *Inorg. Chem.* **1989**, *28*, 3081.
(11) Avshu, A.; Parkins, A. W. *J. Chem. Res. (S)* **1984**, 245.
(12) For **1**, MITHRIL90: Gilmore, C. J. An integrated direct methods computer program. University of Glasgow, Scotland, 1990. For **2**, SAPI91: Fan, H.-F. Structure Analysis Programs with Intelligent Control, Rigaku Corp., Tokyo, Japan, 1991. For **3**, SHELX86: Sheldrick, G. M. *Crystallographic Computing 3*; Oxford University Press: Oxford, U.K., 1985; Vol. 3.

Table 2. Selected Atomic Coordinates and Isotropic Temperature Factors for $[Pt(CN)_2(i\text{-biq})]\cdot 0.5H_2O$

atom	*x*	*y*	*z*	B_{eq},[a] Å^2
Pt	0.64418(5)	0.24778(5)	0.25	5.59(2)
N1	0.521(1)	0.1889(6)	0.25	4.0(4)
N2	0.701(1)	0.1432(7)	0.25	7.8(6)
N3	0.530(2)	0.3920(8)	0.25	5.1(6)
N4	0.839(2)	0.328(1)	0.25	16(1)
C1	0.434(1)	0.2143(8)	0.25	3.8(5)
C2	0.354(1)	0.1704(8)	0.25	3.9(5)
C3	0.260(2)	0.199(1)	0.25	5.9(7)
C4	0.183(2)	0.155(1)	0.25	8.6(9)
C5	0.192(2)	0.077(1)	0.25	8(1)
C6	0.286(2)	0.049(1)	0.25	5.8(7)
C7	0.366(1)	0.0940(9)	0.25	3.9(5)
C8	0.460(1)	0.0664(7)	0.25	3.6(5)
C9	0.532(2)	0.1144(9)	0.25	3.1(5)
C10	0.634(1)	0.0889(8)	0.25	3.3(4)
C11	0.659(1)	0.0173(8)	0.25	4.7(5)
C12	0.757(1)	−0.0014(9)	0.25	5.5(6)
C13	0.786(2)	−0.076(1)	0.25	7.0(8)
C14	0.883(2)	−0.091(1)	0.313(4)	5(1)
C15	0.951(2)	−0.036(1)	0.334(5)	5(1)
C16	0.920(2)	0.033(1)	0.339(6)	7(1)
C17	0.823(2)	0.054(1)	0.315(6)	5(1)
C18	0.791(2)	0.126(1)	0.25	11(1)
C19	0.571(2)	0.3403(9)	0.25	5.2(6)
C20	0.771(2)	0.300(1)	0.25	8.9(9)

[a] $B_{eq} = {}^8/_3\pi^2(U_{11}(aa^*)^2 + U_{22}(bb^*)^2 + U_{33}(cc^*)^2 + 2U_{12}aa^*bb^* \cos\gamma + 2U_{13}aa^*cc^* \cos\beta + 2U_{23}bb^*cc^* \cos\alpha)$.

0.5. Though the N4 atom of a cyanide ligand and the oxygen atom of crystal water also have elongated thermal ellipsoids, they were fixed on the mirror plane and 2-fold axis, respectively, because trials of the Fourier peak separation for the atoms gave worse results on the thermal parameters and the bond lengths and angles. Then calculations of full matrix least-squares refinement under the situation converged nicely with normal bond lengths and angles. The hydrogen atoms were included but not refined. The refinement of the structure of **2** was performed with anisotropic temperature factors for non-hydrogen atoms except for disordered atoms in *N*,*N*-dimethylformamide (C21). The hydrogen atoms of 3,3′-biisoquinoline were included but not refined. It is supposed that there exist two water molecules in the unit cell of the crystal on the basis of the measured density, but their positions cannot be assigned because they are probably highly disordered. All the non-hydrogen atom coordinates of **3** were refined anisotropically. The dimethylformamide molecule in the crystal of **3** was also refined with disordered positions. Further difference Fourier syntheses permitted location of the hydrogen atoms of biisoquinoline ligands, and their coordinates were refined but isotropic temperature factors, B_{iso}, were held fixed. Natural atom scattering factors were taken from the literature.[13] The final *R* indices are listed in Table 1. Positional parameters for significant atoms of the complexes **1**−**3** are in Tables 2−4, respectively. All calculations were performed using the teXsan crystallographic software package of Molecular Structure Corp.

Other Physical Measurements. Absorption spectra were recorded on a Shimazu UV-240 spectrophotometer. Emission spectra were obtained on a Hitachi 850 spectrofluorimeter. Low-temperature emission measurements were performed using an attachment for phosphorescence with a liquid nitrogen dewar. Emission decays were measured on a Horiba NAES-500 or a system constructed with an excimer laser (XeCl; $\lambda = 308$ nm), a monochromator (Nikon G250), and a digital memory (Iwatsu DM-7200). Quantum yields (Φ) of glassy solution were determined by the optically dilute measurements according to the literature.[14] The concentrations of the samples in ethanol−methanol (4:1 (v/v)) were adjusted so as to show the absorbance of *ca*. 0.01 at 360 nm, the excited wavelength (band path = 5 nm). The

Table 3. Selected Atomic Coordinates and Isotropic Temperature Factors for $[PtCl_2(i\text{-biq})]\cdot DMF\cdot H_2O$

atom	*x*	*y*	*z*	B_{eq},[a] Å^2
Pt	0.26988(4)	0.37609(4)	0.37682(7)	2.71(1)
Cl1	0.4589(3)	0.3302(3)	0.5394(5)	4.33(8)
Cl2	0.2926(3)	0.1878(3)	0.2181(5)	5.31(9)
N1	0.2393(8)	0.5420(8)	0.516(1)	2.8(2)
N2	0.1007(9)	0.4268(8)	0.256(1)	2.8(2)
C1	0.314(1)	0.597(1)	0.626(2)	3.3(3)
C2	0.281(1)	0.709(1)	0.735(2)	3.4(3)
C3	0.363(1)	0.768(1)	0.851(2)	4.5(4)
C4	0.323(2)	0.875(1)	0.950(2)	5.9(5)
C5	0.199(2)	0.929(1)	0.935(2)	4.9(4)
C6	0.116(1)	0.877(1)	0.822(2)	4.9(4)
C7	0.153(1)	0.766(1)	0.709(2)	3.4(3)
C8	0.071(1)	0.709(1)	0.575(2)	3.2(3)
C9	0.112(1)	0.602(1)	0.474(2)	2.8(3)
C10	0.039(1)	0.535(1)	0.333(1)	2.6(3)
C11	−0.086(1)	0.576(1)	0.269(2)	3.0(3)
C12	−0.150(1)	0.509(1)	0.131(2)	2.8(3)
C13	−0.277(1)	0.544(1)	0.069(2)	3.7(3)
C14	−0.332(1)	0.476(1)	−0.071(2)	4.2(4)
C15	−0.268(1)	0.367(1)	−0.153(2)	4.3(4)
C16	−0.145(1)	0.327(1)	−0.091(2)	3.5(3)
C17	−0.085(1)	0.399(1)	0.049(1)	2.8(3)
C18	0.040(1)	0.363(1)	0.117(1)	3.0(3)

[a] $B_{eq} = {}^8/_3\pi^2(U_{11}(aa^*)^2 + U_{22}(bb^*)^2 + U_{33}(cc^*)^2 + 2U_{12}aa^*bb^* \cos\gamma + 2U_{13}aa^*cc^* \cos\beta + 2U_{23}bb^*cc^* \cos\alpha)$.

Table 4. Selected Atomic Coordinates and Isotropic Temperature Factors for $[Pt(i\text{-biq})_2](PF_6)_2\cdot 2DMF$

atom	*x*	*y*	*z*	B_{eq},[a] Å^2
Pt	0	0	0	2.466(7)
N1	−0.0780(4)	0.0117(3)	0.1897(6)	2.8(1)
N2	−0.0517(4)	−0.1471(3)	−0.0459(6)	2.8(1)
N3	−0.3500(6)	−0.3344(5)	−0.5727(9)	5.3(2)
C1	−0.0606(6)	0.0860(4)	0.3355(8)	3.2(1)
C2	−0.1389(6)	0.0956(4)	0.4420(8)	3.1(1)
C3	−0.1215(7)	0.1786(5)	0.5933(8)	3.8(1)
C4	−0.2012(8)	0.1857(6)	0.688(1)	4.8(2)
C5	−0.2992(9)	0.1105(6)	0.641(1)	5.2(2)
C6	−0.3175(8)	0.0300(6)	0.495(1)	5.0(2)
C7	−0.2366(6)	0.0204(5)	0.3926(9)	3.7(1)
C8	−0.2459(6)	−0.0632(5)	0.2432(9)	3.6(1)
C9	−0.1653(6)	−0.0689(4)	0.1504(8)	3.0(1)
C10	−0.1473(5)	−0.1598(4)	0.0221(7)	2.8(1)
C11	−0.2020(6)	−0.2534(5)	−0.0130(9)	3.5(1)
C12	−0.1584(6)	−0.3419(4)	−0.1104(8)	3.3(1)
C13	−0.2136(7)	−0.4405(5)	−0.151(1)	4.5(2)
C14	−0.1611(9)	−0.5220(5)	−0.242(1)	5.5(2)
C15	−0.0538(8)	−0.5103(5)	−0.290(1)	4.9(2)
C16	0.0005(7)	−0.4171(5)	−0.2529(9)	4.0(2)
C17	−0.0528(6)	−0.3295(4)	−0.1632(8)	3.0(1)
C18	−0.0036(6)	−0.2309(4)	−0.1292(8)	3.1(1)

[a] $B_{eq} = {}^8/_3\pi^2(U_{11}(aa^*)^2 + U_{22}(bb^*)^2 + U_{33}(cc^*)^2 + 2U_{12}aa^*bb^* \cos\gamma + 2U_{13}aa^*cc^* \cos\beta + 2U_{23}bb^*cc^* \cos\alpha)$.

values of Φ of the samples were calculated according to eq 1, where

$$\Phi_x = \Phi_s(D_x/D_s)(1 - 10^{-A_sL})/(1 - 10^{-A_xL}) \quad (1)$$

D is the integrated area under the corrected emission spectrum, *A* is the absorbance per centimeter at the exciting wavelength, and *L* is the path length of the cell. The subscripts x and s refer to the unknown and standard, respectively. $[Ru(bpy)_3]Cl_2$ was used as a standard ($\Phi = 0.38$).[15] As a test sample, the quantum yield measurement on $[Ru(phen)_3]^{2+}$ (phen = 1,10-phenanthroline) gave the value of 0.533, in good agreement with the literature value (0.58).[15] Emission intensity data for the estimation of the quantum yields were corrected with respect

(13) Cromer, D. T.; Waber, J. T. *International Tables for X-ray Crystallography*; The Kynoch Press: Birmingham, England, 1974; Vol. IV.
(14) (a) Parker, C. A.; Rees, W. T. Analyst **1960**, *85*, 587. (b) Demas, J. N.; Crosby, G. A. *J. Phys. Chem.* **1971**, *75*, 991.
(15) Demas, J. N.; Crosby, G. A. *J. Am. Chem. Soc.* **1971**, *93*, 2841.

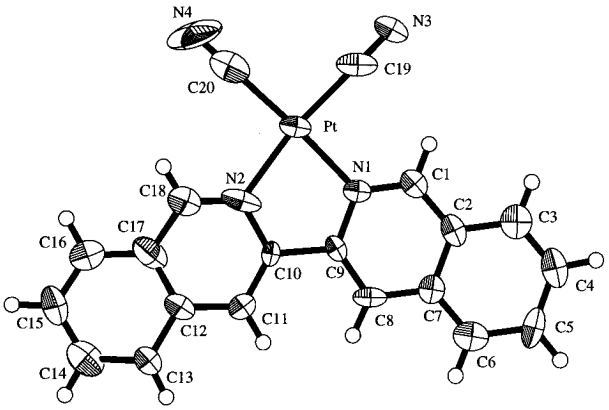

Figure 1. ORTEP drawing of $[Pt(CN)_2(i\text{-biq})]$ (**1**). Thermal ellipsoids are depicted at the 50% probability level.

Table 5. Relevant Bond Lengths (Å) and Angles (deg) and Nonbonded Distances (Å) of the Platinum(II) Complexes

$[Pt(CN)_2(i\text{-biq})]\cdot 0.5H_2O$		$[PtCl_2(i\text{-biq})]\cdot DMF\cdot H_2O$		$[Pt(i\text{-biq})_2](PF_6)_2\cdot 2DMF$	
Pt−N1	2.03(1)	Pt−Cl1	2.296(3)	Pt−N1	2.012(4)
Pt−N2	2.07(1)	Pt−Cl2	2.295(3)	Pt−N2	2.011(4)
Pt−Cl9	1.98(2)	Pt−N1	2.020(9)		
Pt−C20	2.02(3)	Pt−N2	1.993(9)		
N1−C1	1.30(2)				
N1−C9	1.37(2)				
N1−Pt−N2	80.5(6)	Cl1−Pt−C12	89.3(1)	N1−Pt−N2	79.4(2)
N1−Pt−C19	90.8(7)	Cl1−Pt−N1	93.2(3)	N1−Pt−N2′	100.6(2)
N1−Pt−C20	176.3(7)	Cl1−Pt−N2	174.7(3)		
N2−Pt−C19	171.4(8)	Cl2−Pt−N1	176.7(3)		
N2−Pt−C20	95.8(8)	Cl2−Pt−N2	95.2(3)		
C19−Pt−C20	92.9(8)	N1−Pt−N2	82.2(4)		
Pt−C19−N3	179(2)				
Pt−C20−N4	179(2)				
Pt···Pt′	3.34	N1···C11′	3.40(2)	N2···C4′	3.310(9)
O···N4	3.02(2)	N1···C12′	3.40(2)	C1···C2′	3.538(8)
C1···C1′	3.59(1)	N2···C8′	3.46(2)	C1···C7′	3.589(9)
C4···C14″	3.27(3)	C1···C12′	3.55(2)	C3···C9′	3.491(9)
C5···C13″	3.355(4)	C1···C13′	3.51(2)	C3···C10′	3.457(8)
C5···C14″	3.11(3)	C7···C17′	3.47(2)	C4···C18′	3.40(1)
C6···C12″	3.505(8)	C8···C18′	3.35(2)		
C9···C19′	3.484(8)	C9···C10′	3.43(2)		
		C9···C11′	3.50(2)		
		C10···C10′	3.33(2)		
		C9···C15″	3.49(2)		
		C9···C16″	3.52(2)		
		C10···C16″	3.42(2)		
		C10···C17″	3.53(2)		
		C11···C18″	3.53(2)		
		C12···C18″	3.40(2)		

to the sensitivity of the detector by observing the standard spectra of *m*-(dimethylamino)nitrobenzene and 4-(dimethylamino)-4′-nitrostilbene.[16]

Results and Discussion

Structural Description. Table 5 lists relevant bond lengths and angles and nonbonded contacts.

$[Pt(CN)_2(i\text{-biq})]$ (1). Figure 1 shows an ORTEP drawing of **1**. The coordination geometry of platinum is essentially square-planar. Most of atoms in the complex just lie in a crystallographic mirror plane. However, several atoms of the *i*-biq ligand disorder by displacing from the mirror plane, and a tendency of disorder is noticed for a cyanide ligand (see Experimental Section). In the case of $[Pt(CN)_2(bpy)]$, it has been reported that all the atoms are exactly on the mirror plane.[10] Such a difference reflects that biisoquinoline is easy to deform

(16) Lippert, E.; Nägele, W.; Seibold-Blankenstein, I.; Staiger, U.; Voss, W. *Z. Anal. Chem.* **1959**, *17*, 1.

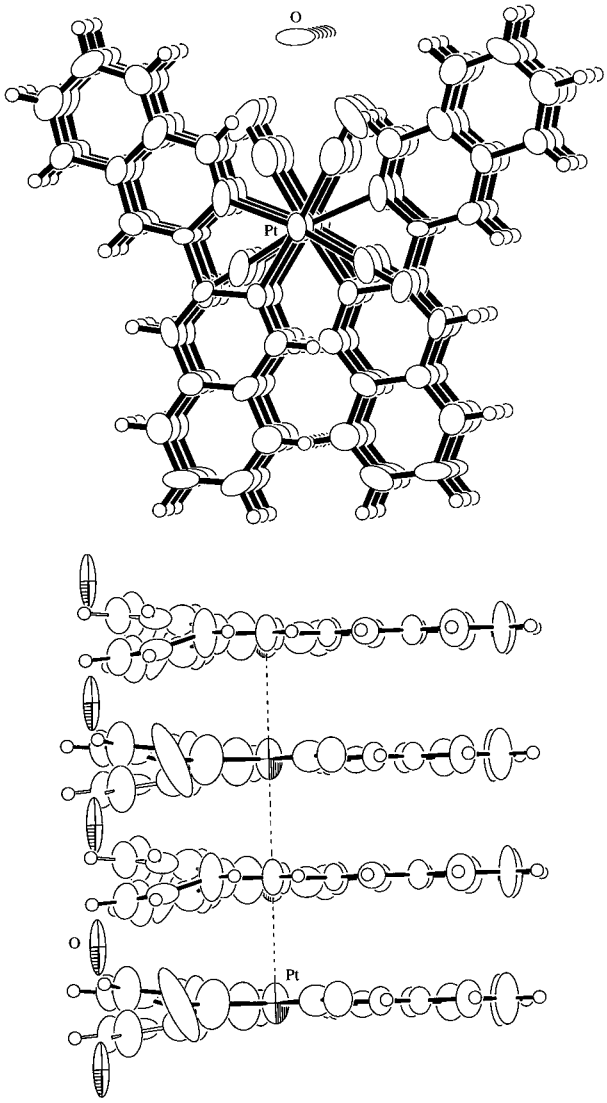

Figure 2. Stacking structure of $[Pt(CN)_2(i\text{-biq})]\cdot 0.5H_2O$: (a, top) top view; (b, bottom) side view.

because of the extended benzene rings in comparison with the bpy ligand. As shown in Figure 2, the platinum complexes are stacked in the crystal to form a columnar structure. The Pt−Pt distance is found to be 3.34 Å. The distance is almost the same as that for the corresponding bpy complex (3.33 Å).[10] However, the stacking pattern differs considerably. In the case of the bpy complexes with metal−metal interactions, two types of stacking pattern are known. One is a columnar stacking of superimposed monomeric units for $[Pt(CN)_2(bpy)]$, and another is an alternating arrangement of monomers for $[PtCl_2(bpy)]$.[4b] The stacking of **1** is unique in that it takes an intermediate form between them. Only half of the ligands (*i.e.*, isoquinolyl units) are arranged closely. The stacked part of the ligand (*i.e.*, the right side of the complex in Figure 2b) is ordered, while the other part (*i.e.*, the left side of the complex in Figure 2b) is disordered vertically. The unstacked part seems to flutter in the extended free space. It is worth noting that a water molecule is located near the CN^- ligands bridging between the complexes in the stack (Figure 2b). The O···N4 distance of 3.02 Å suggests the existence of weak hydrogen bonding. The thermal ellipsoid elongated along the *c* axis is likely to relate to that of the N4 atoms of CN^-. However, as the occupancy factor of the oxygen atom is 0.5, the interaction between the crystal water and the CN^- ligand would not be so strong as it affects the electronic state of the platinum complex.

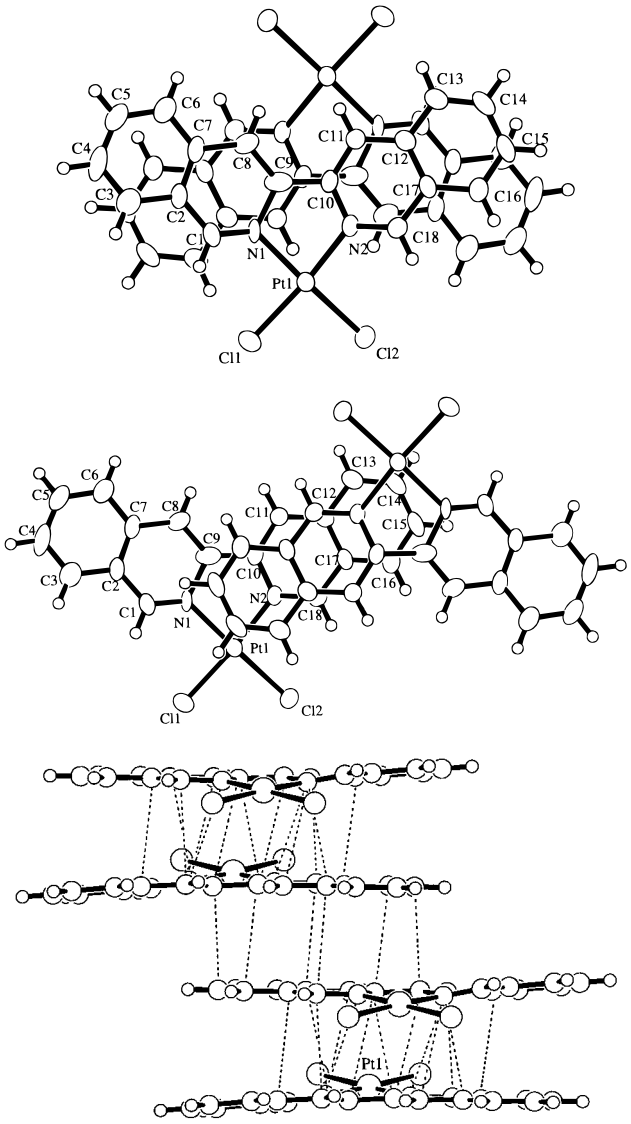

Figure 3. Stacking structure of $[PtCl_2(i\text{-biq})]$ (**2**): (a, top) top view of two adjacent complexes, Pt···Pt = 6.387(1) Å; (b, middle) top view of another pair of adjacent complexes, Pt···Pt = 8.394(1) Å; (c, bottom) side view, dotted lines denote the interatomic distances shorter than 3.5 Å.

$[PtCl_2(i\text{-biq})]$ (2). The complex is almost planar with normal bond lengths and angles though it does not have any crystallographic symmetry such as a mirror plane. In this complex, there cannot be seen any disorder in the *i*-biq ligand differing from the case of **1**. It is because of a completely different stacking structure from that of the dicyano complex. As shown in Figure 3, the stacking occurs on the *i*-biq ligands and the Pt atoms are separated more than 6 Å in the crystal (see the caption of Figure 3). Two kinds of π-stacking geometries are found alternately in the stack. As shown by dotted lines in Figure 3c, among the adjacent *i*-biq ligands in both geometries, many interatomic distances are shorter than 3.5 Å, which is the sum of the van der Waals radius of aromatic carbon. The data are listed in Table 5.

$[Pt(i\text{-biq})_2](PF_6)_2$ (3). Figure 4 shows ORTEP drawings of $[Pt(i\text{-biq})_2]^{2+}$. The most characteristic point in the structure of the bis complex is the distortion from planarity of the *i*-biq ligands, as shown in Figure 4b. It is due to the steric crowding of the α-hydrogens on opposite ligands. The same phenomenon has been reported for the $(bpy)_2$ and $(phen)_2$ complexes of the *trans* geometry (*i.e.*, coplanar coordination).[17] For the *trans*-$(bpy)_2$ complexes, two conformations have been observed. One

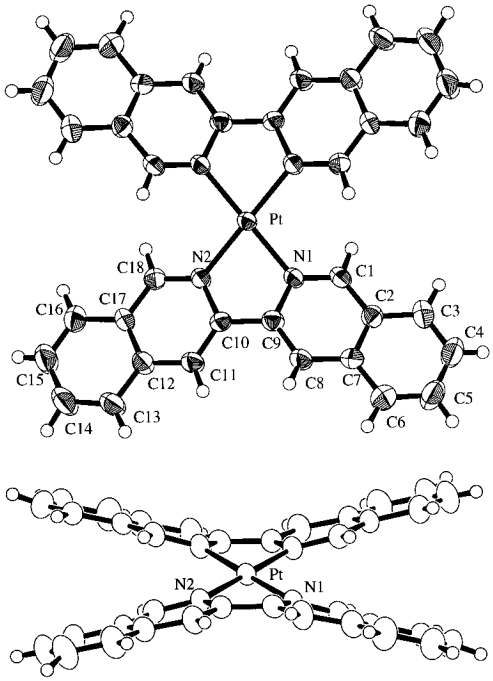

Figure 4. ORTEP drawings of $[Pt(i\text{-biq})_2]^{2+}$. Thermal ellipsoids are depicted at the 50% probability level: (a, top) top view; (b, bottom) side view.

is the bowed conformation in which each ligand is bent in opposite directions, and the other is the twisted conformation in which the opposing bpy ligands are twisted and the coordination plane is deformed tetrahedrally. For more rigid phenanthroline complexes, almost all the complexes of this type take the twisted conformation to relieve the steric hindrance though a unique conformation with tilted ligands from the idealized coordination plane has been reported on the *trans*-$[Ru(phen)_2(py)_2]^{2+}$ complex.[17d] In the case of **3**, the more flexible *i*-biq ligands take on a bowed conformation (Figure 4b). The angle between two isoquinolyl groups is found to be 25°, though each isoquinolyl group in the ligand is almost planar. This angle is larger than any other value reported for this type of deformation in *trans*-$(bpy)_2$ complexes. In the crystal, the complex adopts a slipped-stack structure, keeping van der Waals contacts between parts of adjacent *i*-biq ligands (Figure 5 and Table 5). It is clear that there are no Pt−Pt interactions also in this case: The Pt atoms occupy the lattice points.

Emission and Absorption Properties in Solution. Emission and absorption spectra of complexes **1**−**3** in ethanol/methanol (4:1 (v/v)) dilute solution provide information about electronic states of the monomeric complexes. The spectral data of **1**−**3** and other photophysical data are summarized in Table 6. The lowest electronic absorption bands of these complexes are essentially the same, and they are independent of solvents (chloroform, acetonitrile, *N*,*N*-dimethylformamide, ethanol, *etc.*). Thus, the bands are assigned to a $^1\pi\pi^*$ transition of the *i*-biq ligand. Relatively strong emission was observed for the dilute glassy solutions of these complexes, although the emission at room temperature is too weak to detect as is the case for many platinum complexes in solution. Figure 6a shows emission and excitation spectra of **1** in ethanol/methanol glass at 77 K. The excitation spectrum is consistent with the absorption band at room temperature. The emission spectrum has a typical profile

(17) (a) Hazell, A.; Mukhopadhyay, A. *Acta Crystallogr.* **1980**, *B36*, 1647. (b) Hazell, A.; Simonsen, O.; Wernberg, O. *Acta Crystallogr.* **1986**, *C42*, 1707. (c) Cordes, A. W.; Durham, B.; Swepston, P. N.; Pennington, W. T.; Condren, S. M.; Jensen, R.; Walsh, J. L. *J. Coord. Chem.* **1982**, *11*, 251. (d) Bonneson, P.; Walsh, J. L.; Pennington, W. T.; Cordes, A. W.; Durham, B. *Inorg. Chem.* **1983**, *22*, 1761.

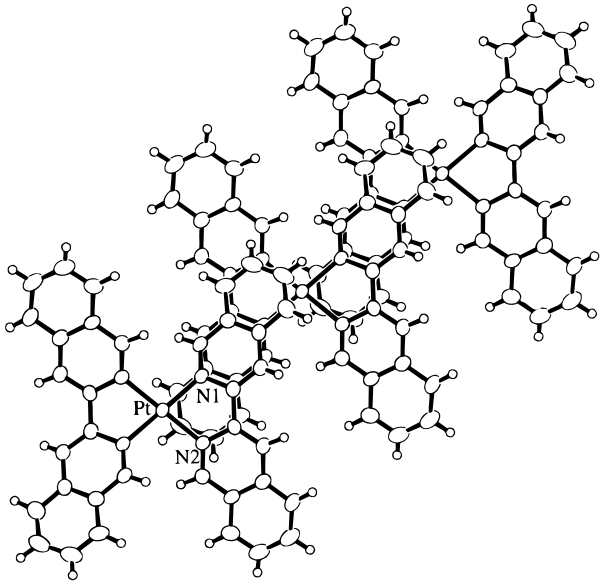

Figure 5. Slipped-stack structure of $[Pt(i\text{-biq})_2]^{2+}$.

Table 6. Emission and Absorption Data for the Platinum(II) Complexes

compounds	absorption[a] λ_{max}/nm (ϵ/(10^4 M^{-1} cm^{-1}))	emission[b] λ_{max}/nm	τ/μs	Φ	k_r[c]/s^{-1}	k_{nr}[c]/s^{-1}
$[Pt(CN)_2(i\text{-biq})]$ (**1**)	375 (2.14)	529	1500	0.111	74	593
$[PtCl_2(i\text{-biq})]$ (**2**)	378 (1.53)	530	331	0.097	293	2730
$[Pt(i\text{-biq})_2](PF_6)_2$ (**3**)	376 (2.25)	530	685	0.049	72	1390

[a] In DMF at room temperature. [b] In ethanol−methanol (4:1 (v/v)) at 77 K. [c] k_r and k_{nr} were calculated from Φ/τ and $(1 - \Phi)/\tau$, respectively.

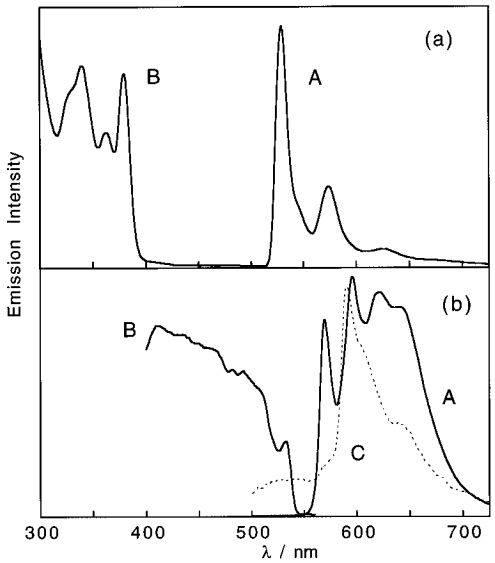

Figure 6. (a) (A) Emission (λ_{ex} = 373 nm) and (B) excitation (λ_{em} = 595 nm) spectra of $[Pt(CN)_2(i\text{-biq})]$ (**1**) in ethanol/methanol (4:1 (v/v)) at 77K; (b) (A) emission (λ_{ex} = 308 nm) and (B) excitation spectra (λ_{em} = 567 nm) spectra and (C) the longest lifetime emission component of the $[Pt(CN)_2(i\text{-biq})]$ crystal at 77 K.

containing a relatively sharp structure, which is characteristic of the $^3\pi\pi^*$ state and is almost the same as those reported for $[Ru(i\text{-biq})_3]^{2+}$.[7,8] However, as shown in Table 6, the emission lifetime of **1** is much longer than that of $[Ru(i\text{-biq})_3]^{2+}$ (*ca.* 100 μs at 77 K).[7] The emission spectra ($^3\pi\pi^*$) in glassy solution for **2** and **3** are almost the same in both energy and profile as those of **1**. Considering the distorted conformation of the *i*-biq ligand in **3** as mentioned above, the sameness in the emission spectra for these complexes indicates that the ligand distortion due to the steric crowding of the complex **3** hardly affects the emissive $^3\pi\pi^*$ in appearance. It is interesting to note that both quantum yield (Φ) and the emission lifetime (τ) for **3** are about half of the corresponding values for **1**. Assuming that the efficiency of populating the emitting state of these complexes is unity, as is the case of Ru(II) and Os(II) photosensitizers,[18] the radiative (k_r) and nonradiative (k_{nr}) rate constants were calculated from $k_r = \Phi/\tau$ and $k_{nr} = (1 - \Phi)/\tau$, respectively (Table 6). Thus, k_{nr} of **3** is estimated to be about twice that of **1**, while their k_r's are comparable. The increase in the nonradiative rate constant for **3** would be explained in terms of the deformation of the *i*-biq ligands. The photophysical features of the dichloro complex, **2**, are different from those of the other complexes (relatively large k_r and k_{nr}). Complex **2** is the first example of a dichloro α-diimine complex, $[PtCl_2(L)]$ (L = α-diimine) having the lowest $^3\pi\pi^*$ emission state. Most of the dichloro complexes show a broad, Gaussian-shaped emission spectrum which is assignable to the emission originating from a ^{3}dd state because of the weak ligand field.[19] The 0−0 energy for $[PtCl_2(bpy)]$ is estimated at 18 900 cm^{-1}, which is comparable to the energy of the $^3\pi\pi^*$ emission for **2** (Table 6). As the ligand field splitting of **2** is expected to be similar to that of $[PtCl_2(bpy)]$, the lowest ^{3}dd state for **2** would occur at almost the same energy as that for $[PtCl_2(bpy)]$. Therefore, the ^{3}dd state would lie just above the $^3\pi\pi^*$ state very closely, which brings about the thermally activated decay, and thus the larger k_{nr} for **2**. As for large k_r for **2**, it is suggested that there is an increase in the mixing of the $^3\pi\pi^*$ emissive state with singlet states. The phenomenon could be explained in terms of the heavy atom effect of chloride ligands in addition to that of the platinum ion.

Emission Properties of the Crystals. As is the case for many platinum complexes with metal−metal interactions, the dicyano complex, **1**, emits intensely in the solid state. The structureless emission spectrum with a maximum at 627 nm at room temperature, which is not observed in solution, is similar to that of the corresponding bpy complex, $[Pt(CN)_2(bpy)]$, which is due to the emission from a $^3d\pi^*[d\sigma^*(Pt) \rightarrow \pi^*(i\text{-biq})]$ state.[10] It is the result that a platinum to bipyridine charge transfer state is considerably lowered in energy by the Pt−Pt electronic interaction. The similarity in the emission spectra of the *i*-biq complex and the bpy complex is consistent with the fact that they have similar Pt−Pt distances (3.34 Å for **1**; 3.33 Å for $[Pt(CN)_2(bpy)]$)[10] and thus, similar metal−metal interactions. The emission maximum and the spectral width are sensitive to the quality of the crystal and temperature. For good crystals of $[Pt(CN)_2(bpy)]$, we observed the large red-shift of the emission maximum from 599 nm at room temperature to 647 nm at 77 K following the shift of the onset from 520 to 565 nm. The result suggests that a shortening of the Pt−Pt distance followed by an increase in the Pt−Pt interaction occurs with lowering temperature. In the case of **1**, however, the emission spectrum of a single crystal at 77 K is much more complicated, as shown in Figure 6b. It is obvious that the spectrum consists of the sharp and broad emission components because the behavior of the emission decay at each peak is different. In fact, as shown with the broken line (C) in Figure 6b, the emission component with the longest lifetime exhibits a typical profile of the $^3\pi\pi^*$(*i*-biq) emission. The emission spectrum appears to have mainly two origins of the $^3\pi\pi^*$ emission (λ_{max}

(18) Demas, J. N.; Taylor, D. G. *Inorg. Chem.* **1979**, *18*, 3177.
(19) Miskowski, V. M.; Houlding, V. H.; Che, C.-M.; Wang, Y. *Inorg. Chem.* **1993**, *32*, 2518.

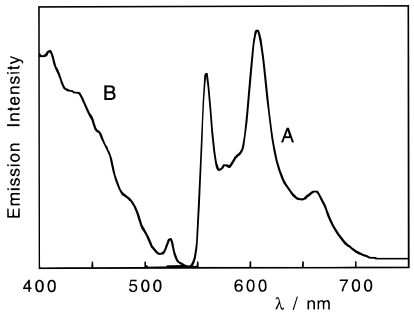

Figure 7. (A) Emission (λ_{ex} = 375 nm) and (B) excitation (λ_{em} = 608 nm) spectra of the [$PtCl_2$(*i*-biq)] crystal at 77 K.

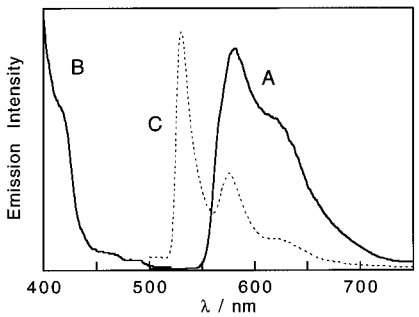

Figure 8. (A) Emission (λ_{ex} = 380 nm) and (B) excitation (λ_{em} = 580 nm) spectra of the [Pt(*i*-$biq)_2$] crystal at 77 K and (C) emission spectrum in ethanol/methanol (4:1 (v/v)).

= 569 and 596 nm). The broad peak around 630 nm corresponds to the $^3d\pi^*$ emission band. The existence of the $^3d\pi^*$ emission as well as the $^3\pi\pi^*$ emission is also confirmed by comparison with the emission spectrum of the crystal of **2**, which exhibits only sharp $^3\pi\pi^*$ emission (*vide infra*). Thus, the single crystal emission of **1** has multiple origins. Their lifetimes were roughly estimated to be *ca.* 300 μs for the $^3\pi\pi^*$ emission and *ca.* 40 μs for the $^3d\pi^*$ emission by means of the analysis of emission decays at several wavelengths. For some Pt(diimine)(dithiolate) complexes in rigid glasses, Eisenberg *et al.* reported similar multiple emission from a $^3\pi\pi^*$ state of the diimine ligand and a metal-to-ligand charge transfer state contributed by a p orbital of sulfur of the dithiolate ligand.[20] As the emitting $^3d\pi^*$ state for **1** arises from the interaction between platinum metals in the crystal, the situation differs from the case of the Pt(diimine)(dithiolate) complexes. However, the phenomenon for **1** indicates that the $^3\pi\pi^*$ state and the $^3d\pi^*$ state are energetically very close in this crystal structure. The $^3d\pi^*$ band does not shift so much from that at room temperature in contrast to the [$Pt(CN)_2$(bpy)] crystal. However, the $^3\pi\pi^*$ bands occur at longer wavelengths compared with that of the glass state, and a corresponding peak can be seen at 532 nm in the excitation spectrum (Figure 6b). The point will be discussed in the succeeding paragraph.

Figure 7 shows the emission and excitation spectra of the crystal of **2** at 77 K. As mentioned above, the emission spectrum (Figure 7A) consists of only a structured component being assignable to the $^3\pi\pi^*$(*i*-biq) emission. Difference in the emission spectral profile from that in the glassy solution could be ascribed to the effect of the reabsorption because it depends on the measuring conditions. The lifetime is roughly estimated to be about 120 μs. As the yellow color of the crystal suggests, the excitation spectrum shown in Figure 7B extends to around 500 nm, which is not observed in the glass state. A peak at 524 nm is assignable to a $^3\pi\pi^*$ band. Thus, the $^3\pi\pi^*$ state in the crystal of **2** as well as **1** is lowered in energy as compared with those in the glassy solutions. This fact is attributable to the intermolecular $\pi-\pi$ interactions on the basis of the crystal structure. Ligand distortion in the crystal (including such local distortion that cannot be detected by X-ray diffraction) could be excluded from the cause of the spectral shift because the emission spectrum for **3** in glassy solution is the same as those for **1** and **2** in the glasses in spite of the essentially distorted structure due to the intramolecular steric crowding of **3**. The peak positions of $^3\pi\pi^*$ in the excitation spectra corresponding to those in the emission spectra indicate that the interaction is not the excimer-type but a stronger one that occurs also in the ground state. For this, the overlap between the filled π-orbitals of the *i*-biq ligands as well as between the empty π^*-orbitals is needed. Observed interatomic distances between the adjacent ligands, though they are the data at room temperature, suggest such strong $\pi-\pi$ interactions for **1** and **2**.

In contrast to the cases of **1** and **2**, the emission spectrum of the crystal of **3** exhibits a fairly broad profile, though it is also red-shifted compared with that of the glassy solution (Figure 8). The spectral features are similar to the $^3\pi\pi^*$ emission of the [Ru(*i*-$biq)_3]^{2+}$ crystal, in which the close contact between the adjacent ligand planes has been also found by X-ray analysis.[8] Miskowski and Houlding reported the broad and red-shifted emission spectrum for the crystal of [$Pt(phen)_2]^{2+}$, which was assigned to the excimeric $^3\pi\pi^*$ emission due to ligand−ligand interactions in the excited state on the basis of the long distance (3.7 Å) between the [$Pt(phen)_2]^{2+}$ complexes in the crystal.[21] Furthermore, excimer formation in fluid solution has been reported for the related complexes, [$Pt(CN)_2$(diimine)] (diimine = 4,7-diphenyl-1,10-phenanthroline, 4,4′-di-*tert*-butyl-2,2′-bipyridine) which have high solubilities.[22,23] The emission spectra of these complexes are red-shifted with increasing concentration, though the excitation spectra do not change. For such dimerization between the excited and ground state complexes in solution, the contribution of the Pt−Pt interaction[22] or $\pi-\pi$ interaction[23] was suggested. In the case of **3**, the complexes in the crystal form a slipped-stack structure overlapping with a part of *i*-biq. Though there are several van der Waals contacts between the adjacent *i*-biq ligands also in the crystal of **3**, as listed in Table 5, the structure seems to generate weaker interactions than those for **1** and **2**. The excitation spectrum (Figure 8B) consistently with the almost colorless feature of the crystal for **3** supports that little interligand interaction takes place in the ground state. Thus, the emission may be regarded as the excimeric one in the sense that it arises from the interaction between the excited complex and the adjacent ground state complex in the crystal. It is interesting to note that complex **3**, [Ru(*i*-$biq)_3]^{2+}$, and [$Pt(phen)_2]^{2+}$ are all dicationic complexes in contrast to **1** and **2**, the neutral ones. The tendency exhibiting such broad spectra in the crystal of the complexes could be related to the charge of the complexes. In the rigid crystal, the electrostatic repulsion possibly prevents the strong interaction among the complexes, but the weak excimeric interaction could occur instead, although, in fluid solution, it seems to be important for excimer formation that the complex is neutral.

Factors Controlling the Crystal Structures. A role of water in dimorphism of [$Pt(CN)_2$(bpy)] has been pointed out by Gillard *et al.*[5] The red form of [$Pt(CN)_2$(bpy)], which has a columnar

(20) (a) Zuleta, J. A.; Bevilacqua, J. M.; Rehm, J. M.; Eisenberg, R. *Inorg. Chem.* **1992**, *31*, 1332. (b) Bevilacqua, J. M.; Eisenberg, R. *Inorg. Chem.* **1994**, *33*, 2913.

(21) Miskowski, V. M.; Houlding, V. H. *Inorg. Chem.* **1989**, *28*, 1529.
(22) Kunkely, H.; Vogler, A. *J. Am. Chem. Soc.* **1990**, *112*, 5625.
(23) Wan, K.-T.; Che, C.-M.; Cho, K.-C. *J. Chem. Soc., Dalton Trans.* **1991**, 1077.

structure with Pt−Pt interaction,[10] changes to the yellow form by hydration. The color indicates the weaker Pt−Pt interaction in the form though the crystal structure has not been known yet. It is suggested that the water molecule in the yellow form interacts with the CN^- ligands through a hydrogen bond. Herber *et al*. have recently reported the hydration behavior of the [Pt-$(CN)_2$L] complexes (L = bpy and substituted bpy) and confirmed the hydrogen bonding between the CN^- ligands and water molecules for the hydrated forms on the basis of the red-shift of the CN stretching bands.[24] The hydrogen bonds weaken the ligand-field strength of CN^-, which causes a decrease in the Pt−Pt interaction. The relationship between the ligand field strength and the Pt−Pt interaction is also understood by comparison of **1** with **2**. In the case of **1**, the red form is stable and can change to yellow powder only in nitric acid. On the other hand, for **2**, the yellow form (*i.e*, the form with no Pt−Pt interaction) has been obtained exclusively. Thus, complex **1**, containing the strong cyanide ligands, prefers the red form, while complex **2**, containing the weak chloride ligands, prefers the yellow form. Similar tendency can be seen for the bpy complexes, though they can take both forms more easily. Consistent with this tendency, the Pt−Pt distance in the red form for the [$Pt(CN)_2$(bpy)] crystal (Pt···Pt = 3.34 Å) is shorter than that for the [$PtCl_2$(bpy)] crystal (Pt···Pt = 3.45 Å). However, the larger distance in the [$PtCl_2$(bpy)] crystal is probably due to the larger Coulombic repulsion of Cl^-. It is recognized that, for square-planar complexes, the stacking structure with Pt−Pt interaction is only slightly stabilized by the configuration interactions between the states concerning the filled d_{z^2} and the empty p_z orbitals (or bands) of the adjacent complexes compared with the monomer.[25] On the other hand, the effect of the metal−ligand distance has been reported on the basis of the extend Hückel MO calculation on $Pt(NH_3)_4$-$PtCl_4$, a model of Magnus' green salt: With a decrease in the metal−ligand distance, and thus an increase in the metal−ligand interaction, the p_z orbital as well as $d_{x^2-y^2}$ particularly increases in energy.[26] Thus, the complexes with a strong ligand field may be advantageous for obtaining stabilization energy based on the interactions. For the *i*-biq complexes, the difference in stability between the red and yellow forms is likely to expand because the intermolecular $\pi-\pi$ stacking interactions are easy to occur on the extended π-system compared with the bpy ligand. As a result, in the case of **2** with the weak ligands, the $\pi-\pi$ stacking structure would be more stable rather than the Pt−Pt stacking structure.

(24) Shih, K.-C.; Herber, R. H. *Inorg. Chem*. **1992**, *31*, 5444.
(25) Krogmann, K. *Angew. Chem., Int. Edn. Engl.* **1969**, *8*, 35.
(26) Interrante, L. V.; Messmer, R. P. *Inorg. Chem*. **1971**, *10*, 1174.

Conclusions

The characteristic stacking structures of the platinum(II) complexes containing *i*-biq and the emission behavior deeply connected with the crystal structures have been clarified. [$Pt(CN)_2$(*i*-biq)] (**1**), which contains strong-field ligands, favors the formation of a columnar structure with Pt−Pt interactions in the crystal. The emission of the crystal at 77 K originates from both $^3\pi\pi^*$(*i*-biq) and $^3d\pi^*(d\sigma^*(Pt) \rightarrow \pi^*$(*i*-biq)] states. On the other hands, [$PtCl_2$(*i*-biq)] (**2**) is arranged to form a π-stacked structure on the *i*-biq ligands and $[Pt(i\text{-biq})_2]^{2+}$ (**3**) takes a slipped-stack structure. The $^3\pi\pi^*$ emission spectra observed for these complexes in the crystal state are red-shifted compared with those in glassy solution. This is attributable to the $\pi-\pi$ intermolecular interactions between the *i*-biq ligands, though their strength is dependent on the crystal structure. Thus, the *i*-biq ligand with larger π-system than bpy has revealed the effect of the intermolecular $\pi-\pi$ interactions definitely and allowed the systematic study of the emission spectroscopy because of the lower-lying $^3\pi\pi^*$ state.

Acknowledgment. The authors thank Dr. Seigo Yamauchi of the Institute for Chemical Reaction Science, Tohoku University, for help with the lifetime measurement. This work was supported by a Grant-in-Aid for Scientific Research (Nos. 06640725, 07215252, 07231219, and 07805079) from the Ministry of Education, Science, Sports and Culture, and was partially supported by a Grant-in-Aid from the Hayashi Memorial Foundation for Female Nature Scientists.

Supporting Information Available: Tables of all non-hydrogen and hydrogen atomic coordinates, all anisotropic thermal parameters, full bond lengths and angles, nonbonded contacts, and least-squares planes and atomic deviations therefrom and text of various characterization parameters for [$Pt(CN)_2$(*i*-biq)]·$0.5H_2O$, [$PtCl_2$(*i*-biq)]·DMF·H_2O, and $[Pt(i\text{-biq})_2](PF_6)_2$·2DMF (35 pages). Ordering information is given on any current masthead page.

IC9507124